Contact-angle hysteresis in solid-on-solid wetting

Phil Attard
Ian Wark Research Institute, University of South Australia, Mawson Lakes, SA 5095, Australia
(Received 24 April 2000; revised manuscript received 1 September 2000; published 19 December 2000)

The spreading of an elastic adhesive sphere on a substrate is calculated using continuum elasticity theory and the van der Waals interaction between the solid surfaces. The deformation and contact area are obtained self-consistently as a function of load. Hysteresis is demonstrated between the loading and the unloading cycles: the receding contact angle exceeds the advancing one. In addition, for a given deformation (flattening), or for a given applied load, the receding contact area exceeds the advancing one. This nonequilibrium phenomenon is velocity dependent and in accord with experiments on adhesion and crack propagation.

DOI: 10.1103/PhysRevE.63.011601 PACS number(s): 68.03.Cd, 62.20.Fe, 68.35.Md

The angles between the phase boundaries at a line of three phase contact depend upon the interfacial energies of the phases. For a liquid drop on a solid in a vapor the Young equation gives

$$\gamma_{sv} = \gamma_{sl} - \gamma_{lv} \cos\theta_{slv}, \tag{1}$$

where the γ are the surface energies of the three interfaces, and where θ_{slv} is the contact angle. The Young equation may be obtained by energy minimization, and it predicts a unique contact angle.

In practice there is not a single value; two values—the advancing and the receding—are generally measured. The contact angle hysteresis is in fact velocity dependent, with the gap between the advancing and receding angles increasing with increasing velocity [1–3]. The existence of hysteresis and dynamic effects indicates that the equilibration of three phase contact occurs over macroscopic time scales, and that the thermodynamic driving force towards equilibrium is small compared to dissipative forces. Accordingly, the Young equation gives the *equilibrium* contact angle, and it would apply for an infinite amount of equilibration. In general energy minimization procedures yield the equilibrium state, but they cannot describe hysteresis or the steady state due to dynamic effects.

Solid particles, such as fluid drops, also deform elastically in response to an applied load or to interactions with a substrate. The area of contact between the two solids grows as the applied load is increased, which is to say that the particle spreads on the substrate. Even at zero load an adhesive particle has a nonzero contact area, so that it may be said to wet the substrate. In view of this obvious analogy between solid particles and fluid drops, one might also expect hysteresis in the case of solid-on-solid wetting.

In the case of solids most attention has focused on their adhesion or pull-off force. The classic JKR equation gives the relationship between adhesion F and surface (or interfacial) energy γ [4],

$$F = -\frac{3}{2}\pi\gamma R, \tag{2}$$

where R is the radius. As in the Young equation, this is derived by constrained free energy minimization, and as an equilibrium result it cannot account for hysteresis in the pull-off force. In practice, large variability and hysteresis is often observed, particularly for soft bodies with large adhesions (e.g., see Refs. [5–11]).

Beyond JKR, which is a contact theory, the deformation of the elastic solids and the pull-off force has been calculated taking into account the finite range of the van der Waals interaction [12–18]. These numerical studies agree that there is hysteresis in the sense that the surfaces jump *in* to contact from a smaller tension than that which causes them to jump *out* of contact. A rather more puzzling hysteresis was revealed by the relatively sophisticated calculations of Attard and Parker [18]. These showed that for soft solids with large adhesions, the loading and unloading branches did not coincide even when the solids were in contact on both branches. This is qualitatively in accord with the experimental evidence [5–11] but it contradicts the widely used JKR result.

Here the mutual spreading of two elastic adhesive solids is reanalyzed in an effort to confirm the earlier results and to identify the physical origin of the hysteresis. Linear elasticity theory is used to obtain the local deformation of the solids due to their interaction. With it the local separation between the surfaces may be written [18]

$$h(r) = h_0(r) - u(r). \tag{3}$$

Here $h_0(r) = h_0 + r^2/2R$ is the surface separation of the undeformed solids at a distance r from the axis. For two spheres with radii R_1 and R_2 the effective radius is $R^{-1} \equiv R_1^{-1} + R_2^{-1}$. The total elastic deformation is given by [18,19]

$$u(r) = \frac{-2}{E}\int_0^\infty p_s[h(t)]k(r,t)t\,dt, \tag{4}$$

where the elasticity parameter is given in terms of Young's modulus and Poisson's ratio of the bodies, $2/E \equiv (1-\nu_1^2)/E_1 + (1-\nu_2^2)/E_2$, and where the kernel is expressible in terms of the complete elliptic integral of the first kind. Finally, the mutual pressure acting between the surfaces is here taken to be a Lennard-Jones representation of the van der Waals attraction

$$p_s(h)=\frac{A}{6\pi h^3}\left[\frac{z_0^6}{h^6}-1\right]. \tag{5}$$

Here A is the Hamaker constant and z_0, which characterizes the range of the short-range repulsion, is the equilibrium separation of planes under zero load. The total load (applied force) is the integral of the Lennard-Jones pressure across the region between the deformed bodies [18]. The value of the surface energy, which is used in making comparison with JKR theory, is $\gamma=A/16\pi z_0^2$. It turns out that the elasticity and adhesion may be combined into the dimensionless parameter [18], $\sigma=\gamma\sqrt{R/z_0^3E^2}$. Large values of σ correspond to soft, adhesive particles.

The problem was discretized for numerical solution using a uniform grid of 1000 nodes. Tests were made with up to 2000 nodes and it was found that the results were not very sensitive to the choice of grid or spacing. The diagonal elements of the kernel matrix were obtained by analytically integrating the logarithmic singularity over the grid width.

As in a loading experiment with controlled displacement, the solids are driven toward each other at a uniform rate beginning at a large separation such that $p_s(h_0)\approx 0$. At each discrete step in position (of size 0.05 nm), new separation, deformation, and pressure profiles, Eqs. (3), (4), and (5), were calculated in turn, with a mixing parameter of up to 0.2. It typically took 500–1000 iterations per step in position for the root mean square change in deformation to be less than 1 pm. Decreasing the convergence parameter to 0.1 pm increased the number of iterations by about an order of magnitude.

This numerical procedure duplicates the experimental protocol of driving the surfaces toward each other at fixed velocity until the maximum load, at which point the motion is reversed. The equilibration time for the deformation and expansion of the contact area is controlled by the drive velocity in the experiments, and by the convergence parameter in the computations. Reducing the speed of the solids is equivalent to increasing the number of iterations per step. The thermodynamic driving force determines the rapidity of convergence toward equilibrium in both the experiments and the computations. In these computations full equilibrium is never attained before the surfaces move on. The motion appears to be overdamped, reaching a quasisteady state that depends upon the velocity of the solids.

Figure 1(A) shows the shape of the sphere as it deforms during loading against a planar substrate. Close inspection of the profiles prior to contact shows that under the influence of the van der Waals attraction the surfaces bulge towards each other by an amount [18] $\delta=-A\sqrt{2R}/8Eh^{5/2}$. At a finite separation the surfaces jump into contact due to an elastic instability [14,15], the rate of energy decrease due to the steep gradient of the van der Waals attraction exceeds the rate of energy increase of elastic deformation at a critical separation [18] $h^*=(3A\sqrt{2R}/8E)^{2/7}$.

Once in contact the surfaces appear flat, and on the scale of the figure there is a relatively sharp transition between the contact and noncontact regions. Accordingly, contact was here defined as a local separation less than $1.1z_0=0.55$ nm.

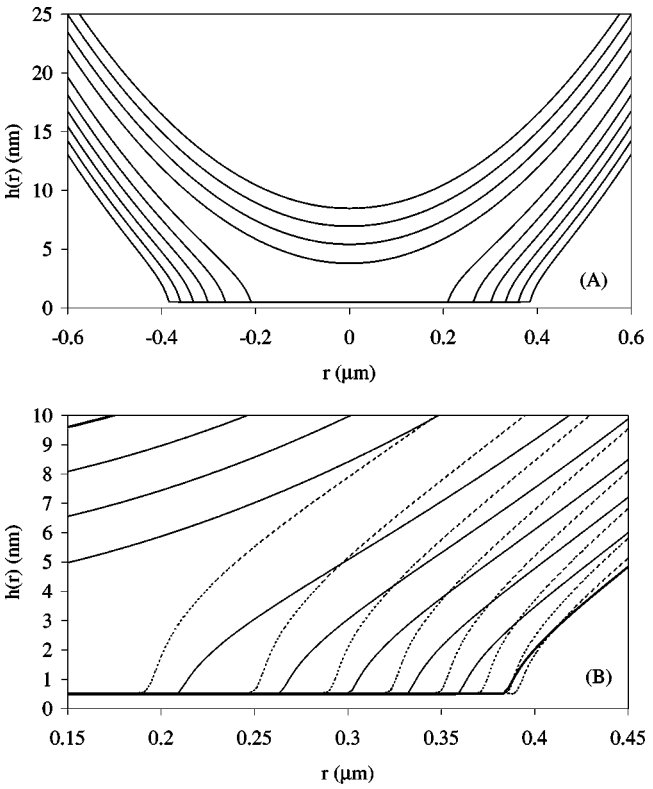

FIG. 1. (A) The shape of an elastic sphere against a flat during loading ($R=10$ μm, $A=10^{-19}$ J, $z_0=0.5$ nm, and $E=3\times10^8$ N m^{-2}, which give $\gamma=7.96$ mN m^{-1} and $\sigma=7.50$). The curves are snapshots taken every 1.5 nm change in position, starting at $h_0=8.5$ nm at the top where the sphere is undeformed. (B) The loading (solid curves) and unloading (dashed curves) at the same positions as in (A). The shapes are coincident (bold solid curves) at the turning point at $h_0=-5$ nm, and at the furthest position from contact at $h_0=8.5$ nm. Note that the receding contact area is greater than the advancing at the corresponding position, and that the contact area at $h_0=-3.5$ nm for unloading is actually greater than at the turning point at $h_0=-5$ nm.

Other definitions of contact lead to qualitatively similar conclusions. As the solids are pushed together the contact area expands, and the neck region becomes less pronounced. In the case shown, the contact radius ranges from 0.2 μm just after the jump into contact to 0.4 μm at the turning point.

Figure 1(B) compares in detail the surface profiles on the loading and the unloading branches. At any given position h_0, the contact area is greater on the unloading branch than on the loading branch. Indeed, after the direction of motion of the solids has been reversed, the contact area continues to expand for a short time. This is due to the fact that the contact area is still growing toward its equilibrium value when the load is reversed. The surfaces remain in contact on the unloading branch *after* the position h_0^* at which they jumped into contact on approach.

It can be seen in Fig. 1(B) that during unloading the sphere is more ''stretched'' than during loading. The exterior angle between the tangent of the deformed sphere (measured in the apparently linear asymptotic region) and the planar substrate is $\theta_{1v2}=49.7$ mrad on approach and 53.7 mrad on

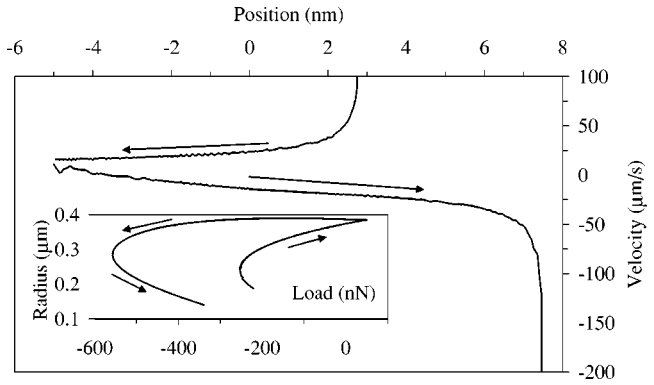

FIG. 2. The velocity of the contact radius as a function of the position h_0 of the sphere of Fig. 1 with a driving velocity $\dot{h}_0 = 1$ μm/s. The speed of the contact line is simply the change in radius between successive drive steps, times the drive velocity, divided by the step length. The zero of position corresponds to contact of the undeformed sphere, and positions prior to contact have a positive value. Inset. The advancing and receding contact radius as a function of load.

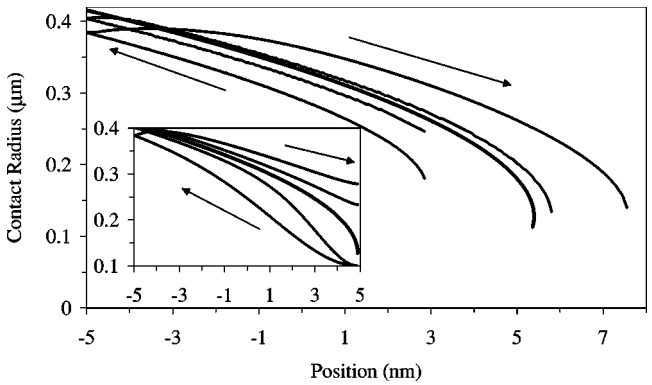

FIG. 3. The contact radius as a function of position h_0 for the parameters of Fig. 1. The convergence parameter was $\epsilon = 1$ and 0.1 pm for the outer and inner curves, respectively. The single bold curve is the JKR equilibrium prediction. Inset. The dynamic JKR theory for a driving velocity of 1 μm/s and drag coefficient of $b = 0.3$ and 0.1 g/s, for the outer and inner curves, respectively.

separation. (The angle made by an undeformed sphere would be about 25 mrad.) That is, the receding contact angle is greater than the advancing one.

The velocity of the contact line is plotted in Fig. 2 for the case when the sphere is driven with velocity $\dot{h}_0 = \pm 1$ μm/s. (The drive velocity is an independently specified variable in the computations and in the experiments that they mimic.) The initial high rate of expansion of the contact area following the jump into contact slows to a relatively steady value ($\approx$20 μm/s) as the load is increased. Immediately following the turn around the velocity briefly remains positive (continued expansion) before the contact area shrinks at an increasing rate. At the point of maximum tension, the velocity of the contact line is approximately -25 μm/s, and by the minimum contact area it is moving at over -100 μm/s.

The inset to Fig. 2 shows the contact radius as a function of load for both the loading and the unloading branches. On loading, while the contact radius monotonically increases as the bodies are driven toward each other, the load initially decreases (becomes more negative), following the jump into contact, and then increases. The fact that the contact area grows to about 0.37 μm, where it would remain with no applied load, justifies these two solids being described as mutually ''wetting.'' The hysteresis between the loading and the unloading branches is quite marked. At the same load the contact radius is greater on the unloading branch than on the loading branch. Upon unloading, the contact area does not begin to decrease significantly until the tension has increased to several hundred nano-Newtons. The extreme tension of 557 nN, which occurs at a contact radius of 0.29 μm, represents the pull-off force. In an experiment with controlled load, this is the last stable point before the surfaces jump out of contact. In the present calculations the position rather than the load is controlled, and results for the unstable region in which the radius decreases with decreasing tension are also given. The smallest contact radius exhibited, 0.14 μm, at a tension of 339 nN, represents the absolute limit at which the surfaces can remain in contact.

Calculations have also been performed varying the maximum applied load (not shown). In general the unloading paths do not coincide, and in particular the pull-off force increases with increasing applied load, confirming previous results [18]. For large enough maximum loads, the unloading curves tend to coincide around the pull-off point and on the unstable portion of the curve, which implies a saturation in the pull-off force with maximum load.

The effect of the convergence parameter on the hysteresis is explored in Fig. 3, which plots the contact radius against the position (undeformed separation) for two values $\epsilon = 1$ and 0.1 pm. The number of iterations for each drive step increased by about an order of magnitude. During loading, the contact radius at a given position is larger in the system that has been given longer to equilibrate at each drive step. Conversely, during unloading, the contact area is smaller in the more slowly moving system. The result of this is that the hysteresis decreases with increasing equilibration time.

Also shown in Fig. 3 is the JKR prediction for the contact radius. As the driving speed of the solids is decreased and the equilibration time is increased, the contact radius on each branch approaches the JKR prediction. This supports the conclusion that JKR theory, similar to the Young equation, is an equilibrium theory that might possibly be applicable to a static measurement, if such a thing were possible. Conversely, the JKR theory cannot predict the adhesion or deformation in the case of hysteresis, which occurs due to the restricted equilibration of solids driven with nonzero velocities.

The inset of Fig. 3 shows steady state dynamic calculations in which the force driving the change in contact radius is balanced by a drag force proportional to its velocity, $b\dot{a} + \partial U(\delta, a)/\partial a = 0$ [20]. Here U is the Hertz and Johnson elastic energy, expanded to second order about equilibrium, and b is a drag coefficient. Although this is a contact theory, which is not as realistic as the van der Waals calculations, it is a fully dynamic theory that uses a common model of fric-

tion and energy dissipation. It can be seen that a smaller drag coefficient decreases the hysteresis between loading and unloading. Zero drag (or equivalently zero driving velocity) yields the equilibrium JKR prediction. The similarity with the hysteresis displayed in the main figure supports the argument that the iteration procedure is quasidynamic and that the motion depends upon the thermodynamic distance from equilibrium.

The present results qualitatively differ from the classic JKR theory for the adhesion of elastic solids in that they indicate the presence of hysteresis between loading and unloading. Hysteresis was found in the shape and in the contact area and angle, and identified as the cause of the load-position hysteresis found in earlier work [18]. The contact area is in general greater upon unloading than at the equivalent point on the loading branch, that the shape of the surfaces differs on the two branches, and that the exterior contact angle is greater for the receding contact line than for the advancing one.

The hysteresis is not due *per se* to the finite range of the van der Waals attraction, or to the nonlinear nature of the elasticity equations. Rather, the classic equations of contact mechanics [4], and the more recent numerical calculations [12–17], were found to represent the equilibrium result (i.e., the constrained free energy minimum), whereas the present results represent the steady state approach to equilibrium. That is, the hysteresis depends upon the dynamics of the system, namely, the limited equilibration time allowed. The deformation appears to approach its equilibrium value at a steady rate determined by the balance of thermodynamic (elastic and surface) forces and dissipative forces. The former decrease with decreasing distance from equilibrium, and the latter increase with velocity, which damping effect slows the speed of the contact line and prevents static equilibrium being achieved. This viscoelastic effect, which is present in all solids, has measurable consequences in the soft systems with large adhesions analyzed here. The hysteresis can be decreased by using slower driving velocities (more iterations per drive step) since this permits greater convergence towards equilibrium. It is not possible to perform a strictly static calculation (nor a static measurement) but it appears that JKR theory is the limiting result for infinitely slow driving velocities.

The existence of contact angle hysteresis and the dependence of the pull-off force on the maximum applied load found here are consistent with measured data in a broad range of solid-solid systems (e.g., see Refs. [5–11]). In those cases where the dynamics have been controlled, (and also other adhesion and peeling experiments [21,22]), the phenomena has been shown to depend upon the speed of the measurements. Such hysteresis and its dynamic nature are of course well-known for liquid drops and for gas bubbles in contact with a solid [1–3]. Speculation about the cause of the hysteresis, for both fluids and solids, usually invokes physical roughness, chemical heterogeneity, or molecular rearrangement. The present calculations for ideal model surfaces suggest rather that these are not necessary for wetting hysteresis, but rather that it is a general phenomenon whose origin lies in the nature of elastic deformation of the solid and the macroscopic time scales for it to equilibrate.

The support of the Australian Research Council through the Special Research Center for Particle and Material Interfaces at the Ian Wark Research Institute is gratefully acknowledged.

[1] P. G. de Gennes, Rev. Mod. Phys. **57**, 827 (1985).
[2] R. A. Hayes and J. Ralston, J. Colloid Interface Sci. **159**, 429 (1993).
[3] R. G. Cox, J. Fluid Mech. **357**, 249 (1998).
[4] K. L. Johnson, K. Kendall, and A. D. Roberts, Proc. R. Soc. London, Ser. A **324**, 301 (1971).
[5] M. D. Pashley and J. B. Pethica, J. Vac. Sci. Technol. A **3**, 757 (1985).
[6] R. G. Horn, J. N. Israelachvili, and F. Pribac, J. Colloid Interface Sci. **115**, 480 (1987).
[7] N. A. Burnham and R. J. Colton, J. Vac. Sci. Technol. **7**, 2906 (1989).
[8] Y. L. Chen, C. A. Helm, and J. N. Israelachvili, J. Phys. Chem. **95**, 10736 (1991).
[9] M. Tirrell, Langmuir **12**, 4548 (1996).
[10] M. Deruelle, H. Hervet, G. Jandeau, and L. Leger, J. Adhes. Sci. Technol. **12**, 225 (1998).
[11] F. J. Schmidtt, T. Ederth, P. Weidenhammer, P. Claesson, H. J. Jacobasch, J. Adhes. Sci. Technol. **13**, 79 (1999).
[12] V. M. Muller, V. S. Yushchenko, and B. V. Derjaguin, J. Colloid Interface Sci. **77**, 91 (1980).
[13] B. D. Hughes and L. R. White, Quarterly J. Mech. Appl. Math. **32**, 445 (1979).
[14] J. B. Pethica and A. P. Sutton, J. Vac. Sci. Technol. A **6**, 2490 (1988).
[15] J. R. Smith, G. Bozzolo, A. Banerjea, and J. Ferrante, Phys. Rev. Lett. **63**, 1269 (1989).
[16] J. L. Parker and P. Attard, J. Phys. Chem. **96**, 10 398 (1992).
[17] J. A. Greenwood, Proc. R. Soc. London, Ser. A **453**, 1277 (1997).
[18] P. Attard and J. L. Parker, Phys. Rev. A **46**, 7959 (1992); Phys. Rev. E **50**, 5145(E) (1994).
[19] L. D. Landau and E. M. Lifshitz, *Theory of Elasticity*, 2nd ed. (Pergamon, London, 1970).
[20] P. Attard (unpublished).
[21] D. Maugis and M. Barquins, J. Phys. D **11**, 1989 (1978).
[22] M. Deruelle, H. Hervet, G. Jandeau, L. Leger, J. Adhes. Sci. Technol. **12**, 225 (1998).